



Contents lists available at ScienceDirect

Ocean Modelling

journal homepage: www.elsevier.com/locate/ocemod

A boundary-value problem for the parameterized mesoscale eddy transport

Raffaele Ferrari^{a,*}, Stephen M. Griffies^b, A.J. George Nurser^c, Geoffrey K. Vallis^d^aMassachusetts Institute of Technology, Cambridge, USA^bNOAA Geophysical Fluid Dynamics Laboratory, Princeton, USA^cSouthampton Oceanography Centre, Southampton, UK^dGFDL and Princeton University, Princeton, USA

ARTICLE INFO

Article history:

Received 28 July 2009

Received in revised form 13 January 2010

Accepted 18 January 2010

Available online xxxx

Keywords:

Mesoscale

Eddy

Parameterization

Turbulence

Ocean

Modelling

ABSTRACT

We present a physically and numerically motivated boundary-value problem for each vertical ocean column, whose solution yields a parameterized mesoscale eddy-induced transport streamfunction. The new streamfunction is a nonlocal function of the properties of the fluid column. It is constructed to have a low baroclinic mode vertical structure and to smoothly transition through regions of weak stratification such as boundary layers or mode waters. It requires no matching conditions or regularization in unstratified regions; it satisfies boundary conditions of zero transport at the ocean surface and bottom; and it provides a sink of available potential energy for each vertical seawater column, but not necessarily at each location within the column. Numerical implementation of the methodology requires the solution of a one-dimensional tridiagonal problem for each vertical column. To illustrate the approach, we present an analytical example based on the nonlinear Eady problem and two numerical simulations.

© 2010 Elsevier Ltd. All rights reserved.

1. Introduction

Geostrophic eddies dominate the kinetic energy of the World Ocean. These eddies stir and mix heat, salt, and other climatologically relevant tracers throughout the oceans. Ocean climate models typically use grid sizes that are too coarse to explicitly resolve geostrophic eddies, and so eddy effects must be parameterized in such models.

The parameterization of mesoscale eddies is often framed as the parameterization of an eddy-induced transport streamfunction, Ψ . A commonly used parameterized streamfunction is that proposed by Gent and McWilliams (1990) and Gent et al. (1995) (referred to as “GM” in the following), in which the streamfunction is given by

$$\Psi^{\text{GM}} = -\kappa \mathbf{S} \wedge \hat{\mathbf{z}}, \quad (1)$$

where κ is an eddy diffusivity, $\mathbf{S} = -\nabla_z \rho / \partial_z \rho$ is the slope of the neutral direction relative to the horizontal (as discussed in Appendix A.2, ρ is the locally referenced potential density and ∇_z is the horizontal gradient operator), and $\hat{\mathbf{z}}$ is the vertical unit vector. Tracer fields are then advected by the velocity

$$\mathbf{v}^{\text{GM}} = \nabla \wedge \Psi^{\text{GM}}, \quad (2)$$

in addition to the Eulerian velocity resolved by the model grid.

* Corresponding author. Address: Massachusetts Institute of Technology, Department of Earth, Atmospheric, and Planetary Sciences, Cambridge, USA. Tel.: +1 617 253 1291; fax: +1 617 253 4464.

E-mail addresses: ferrari@mit.edu (R. Ferrari), stephen.griffies@noaa.gov (S.M. Griffies), G.Nurser@soc.soton.ac.uk (A.J. George Nurser), gkv@princeton.edu (G.K. Vallis).

Various theories have been proposed to determine the eddy fluxes and eddy diffusivity (e.g., Held and Larichev, 1996; Visbeck et al., 1996; Smith and Vallis, 2002; Eden and Greatbatch, 2008), with some suggesting that the fluxes should be a function of the vertically integrated stratification or even a function of the three-dimensional flow. However, even if the diffusivity has become a nonlocal function of the vertical density structure, the streamfunction Ψ^{GM} has generally remained a local function of the neutral slope at each point in the ocean in most current parameterizations.

Although the recipe of Eqs. (1) and (2) seems unambiguous, in practice it can be difficult to compute the streamfunction in realistic simulations admitting arbitrary vertical stratification and satisfying $\Psi^{\text{GM}} = 0$ at the top and bottom boundaries. Methods used to handle such issues are summarized in Griffies (2004), with these methods typically requiring steps to smoothly match the streamfunction across boundary layers, as well as the imposition of a somewhat arbitrary cap on the nominal value of the neutral slope used to construct the streamfunction. These methods are straightforward mathematically, yet can be sensitive to numerical details, and generally lack a sound physical justification. More recently, however, Ferrari et al. (2008) provided a physical rationale for transitioning the streamfunction, via the use of matching conditions, from the stratified interior into weakly stratified boundary layers at the ocean surface and bottom. Danabasoglu et al. (2008) provide model examples where this approach greatly improves the simulation as compared to alternative approaches. They report a reduced sensitivity to interior tapering by allowing a large value of the maximum slope and they provide a capability for handling

boundary layer matching conditions without inordinate numerical difficulties.

Motivated by theories for eddy fluxes that are nonlocal in the vertical, we introduce a new parameterized eddy-induced streamfunction that is determined as the solution to a boundary-value problem for each vertical ocean column. Through theoretical and numerical analysis, we show how the new streamfunction is related to the GM-streamfunction Ψ^{GM} traditionally used in ocean models, and how it naturally transitions through an arbitrary number of boundary layers, without the need to introduce matching conditions or regularization. The approach is similar to that taken in Ferrari et al. (2008), but it generalizes it to the full water column. Additionally, we identify an important area where the new streamfunction differs from Ψ^{GM} . Namely, for a nonlinear Eady problem, eddy fluxes from the new streamfunction match those from theory and process simulations, whereas Ψ^{GM} is singular in the absence of externally specified tapering or matching conditions.

The remainder of this paper consists of the following sections. In Section 2, we review elements of the eddy parameterization problem from the perspective of the tracer equation in a Boussinesq fluid. This section serves to motivate the boundary value problem proposed in Section 3. Section 4 examines the properties of the boundary-value problem, and Section 5 considers some analytic and numerical examples. We close the main portion of the paper with discussion and conclusions in Section 6. Appendices discuss certain technical details.

2. Eddy-induced transport

As noted in the introduction, it is common to parameterize the subgrid scale (SGS) stirring of tracers by mesoscale eddies through a non-divergent eddy-induced velocity, which may be written as the curl of a vector streamfunction, $\mathbf{v}^* = \nabla \wedge \Psi$. Because the velocity $\mathbf{v}^* = (\mathbf{u}^*, w^*)$ is non-divergent, it has only two functional degrees of freedom and one may therefore choose a gauge to represent the vector streamfunction, commonly chosen so that the streamfunction has only horizontal components:

$$\Psi = (\Psi^{(x)}, \Psi^{(y)}, 0). \quad (3)$$

We find it convenient in much of this paper to write the vector streamfunction corresponding to existing mesoscale parameterizations as

$$\Psi = \Upsilon \wedge \hat{\mathbf{z}}, \quad (4)$$

where Υ is the parameterized eddy-induced transport. The eddy-induced velocity is then given by

$$(\mathbf{u}^*, w^*) = (\partial_z \Upsilon, -\nabla \cdot \Upsilon). \quad (5)$$

Appendix A.2 summarizes the relation between the eddy-induced transport, the eddy-induced vector streamfunction, and the eddy-induced meridional overturning streamfunction.

2.1. Relating Υ to eddy fluctuations

Relations between the parameterized eddy-induced transport Υ and subgrid-scale fluctuations depend on how one chooses to partition the tracer and velocity into eddy and mean. Two methods are commonly used, the Transformed Eulerian Mean (TEM) and Temporal Residual Mean (TRM). The TEM formalism has been used extensively in the literature on quasi-geostrophic turbulence, and this link will be used to motivate our choice for the vertical structure of the eddy transport in Section 2.2. Although the two methods return different expressions for large amplitude eddies, the differences are second order for geostrophic eddies. We focus on the TEM formalism here, and present elements of TRM in Appendix A.1.

The TEM formalism is based on averaging the equations in (x, y, z) coordinates. The expression for the transport resulting from subgrid scale eddy motions is derived in Andrews and McIntyre (1978), but it offers little insight for developing parameterizations. Progress is made by assuming that the subgrid scale motions satisfy the quasi-geostrophic (QG) approximation, and in the QG limit the expression for the eddy induced transport reduces to

$$\Upsilon^{\text{TEM}} \approx \frac{\langle \mathbf{u}' \rho' \rangle}{|\partial_z \rho|}, \quad (6)$$

where ρ' is the fluctuating density, and the angle bracket is an averaging operator taken at a fixed Eulerian depth (see, e.g., Plumb, 1990; Plumb and Ferrari, 2005; Ferreira and Marshall, 2006; Zhao and Vallis, 2008; Ferrari et al., 2008).

2.2. Eddy fluxes and low baroclinic modes

The tendency of geostrophic turbulence is to transfer energy to graver (larger) vertical scales (a process commonly known as *barotropization*), as well as graver horizontal scales. This energy transfer is a consequence of the analogy between quasi-geostrophic flow and two-dimensional flow (Charney, 1971). Although barotropization is inhibited in the presence of non-uniform stratification (Smith and Vallis, 2001), numerical simulations indicate that even with fairly realistic profiles of stratification, the quasi-geostrophic potential vorticity flux is dominated by grave vertical scales. The rationalization is that the potential vorticity flux $\langle \mathbf{u}' q' \rangle$ is largely the result of stirring of the low mode potential vorticity gradients by barotropic velocity fluctuations \mathbf{u}'_0 . In fact the flux could be well modelled by considering contributions from only the first baroclinic mode (Smith and Vallis, 2002), and it is this result that largely motivates our parameterization. Notice that we are not contending that the quasi-geostrophic potential vorticity fluxes cannot be dominated by high baroclinic structures; Smith and Vallis (2002) show that one can contrive stratification profiles where this happens. Our contention is that for typical ocean stratification profiles, the bulk of the quasi-geostrophic potential vorticity flux is captured by the first few baroclinic modes. Furthermore, on scales larger than the deformation radius but smaller than the planetary scale, the quasi-geostrophic potential vorticity flux is dominated by the thickness flux and so related to the density flux to a good approximation by (e.g., Treguier et al., 1997; Vallis, 2006)

$$\langle \mathbf{u}' q' \rangle \approx f \frac{\partial}{\partial z} \frac{\langle \mathbf{u}' \rho' \rangle}{\partial_z \rho} = -f \partial_z \Upsilon^{\text{TEM}}, \quad (7)$$

where f is the Coriolis parameter and the last step uses Eq. (6), assuming a stable stratification where $|\partial_z \rho| = -\partial_z \rho$. Given the low mode structure of potential vorticity fluxes, relation (7) also means that density fluxes have a low-mode vertical structure. We take this phenomenology as motivation to construct our proposed boundary-value problem so that low baroclinic modes dominate the parameterized eddy-transport.

A limitation of this approach is that the dominance of low baroclinic modes in the quasi-geostrophic potential vorticity flux has been demonstrated in models that ignore surface fluxes of density. The simulations of Smith and Vallis (2002), e.g., set the density to a constant at the boundary. Recent results (e.g., Klein et al., 2008) suggest that new modes are excited when density is not uniform at the surface. But the problem is still poorly understood, and these complications are left for a future study. Here the goal is to parameterize eddy mixing associated with low baroclinic modes associated with interior ocean dynamics.

2.3. Surface and bottom boundary conditions for Υ

Homogeneous Dirichlet boundary conditions are employed for parameterizations of the mesoscale eddy-induced transport Υ (see Gent et al., 1995; McDougall and McIntosh, 2001), so that

$$\Upsilon(\eta) = \Upsilon(-H) = 0. \quad (8)$$

We list three elements of this boundary condition important for mesoscale eddy closures.

- The boundary condition yields a vanishing vertical integral for the horizontal component \mathbf{u}^* to the eddy-induced velocity, thus ensuring that the mesoscale eddy transport has a zero barotropic component.
- The boundary condition further enforces a zero vertically integrated flux of eddy potential vorticity as per Eq. (7), so that the eddies act only to redistribute momentum within the column.
- The TRM formalism (McDougall and McIntosh, 2001) and Appendix A.1) shows that this boundary condition results from kinematic constraints on flow approaching a geometric boundary such as the ocean surface or bottom.

Although the boundary conditions (8) are of fundamental importance, the parameterized eddy-induced transport from Gent et al. (1995),

$$\Upsilon^{\text{GM}} = -\kappa \mathbf{S}, \quad (9)$$

does not naturally vanish at the ocean surface or bottom, since neither the neutral slope nor the diffusivity necessarily vanish at these boundaries. Consequently, various “tapering” methods have been used to bring Υ^{GM} to zero at the boundaries (e.g., Griffies, 2004). This is typically done by tapering κ so that it vanishes smoothly at the boundaries. To maintain stability of the simulation, these methods must also regularize Υ^{GM} in regions of weak stratification where $N^2 \rightarrow 0$, often associated with boundary layers. It has been found that somewhat arbitrary details of the regularization can produce widely varying simulation features (Gnanadesikan et al., 2007; Ferrari et al., 2008; Farneti et al., in press), as might be expected since the methods affect how the mesoscale closure interacts with mixed layer processes.

It should be noted that as the surface is approached, diabatic effects become important because of air-sea interaction, and so a full parameterization of eddy effects should not be purely advective (e.g., Treguier et al., 1997). Non-advective effects may be included by introducing a down-gradient horizontal diffusive flux of tracer near the upper boundary, in addition to the eddy-induced transport arising from eddy stirring. In our experience the introduction of a horizontally aligned diffusive flux does not reduce the sensitivity of the simulation to the chosen tapering scheme used for the parameterized eddy transport. For the rest of the paper we focus on the parameterization of adiabatic stirring processes parameterized by the eddy-induced transport.

3. A boundary-value problem for the transport

In this section, we propose a one-dimensional boundary-value problem for the eddy-induced transport, to be solved on each vertical ocean column, that satisfies the two key properties identified above. That is, the new parameterized transport satisfies homogeneous Dirichlet boundary conditions at the ocean surface and bottom, and its vertical structure is dominated by low baroclinic modes.

3.1. An expansion in terms of baroclinic modes

We first consider the possibility of expanding the parameterized transport in terms of ‘vertical velocity’ eigenmodes, $S_m(z)$, from the linearized primitive equations (see Appendix B for more details). These eigenmodes satisfy the equation

$$\left(c_m^2 \frac{d^2}{dz^2} + N^2 \right) S_m = 0, \quad (10a)$$

$$S_m(0) = S_m(-H) = 0, \quad (10b)$$

and provide a complete basis for any piecewise continuous and bounded function that vanishes at the boundaries, like Υ (see Appendix B for more discussion of the completeness of the baroclinic modes). The squared buoyancy frequency is given by $N^2 = -(g/\rho_o) \partial_z \rho$, where ρ is the locally referenced potential density, and ρ_o is a constant reference density associated with the Boussinesq approximation. The parameterized transport may thus be written

$$\Upsilon = \sum_{m=1}^{\infty} S_m(z) \Upsilon_m(x, y, t). \quad (11)$$

The expansion coefficients $\Upsilon_m(x, y, t)$ are determined by the orthogonality condition maintained by S_m (see Eq. (58c) in Appendix B), which leads to

$$\Upsilon = \frac{1}{g} \sum_{m=1}^{\infty} S_m(z) \left(\int_{-H}^0 dz' \Upsilon N^2 S_m \right). \quad (12)$$

We now specialize the expansion (12) by considering a modal representation of the Gent et al. (1995) eddy-induced transport, in which case

$$-N^2 \Upsilon^{\text{GM}} = N^2 \kappa \mathbf{S} = (g/\rho_o) \kappa \nabla_z \rho, \quad (13)$$

using the expression (48c) (see Appendix A.2) for the neutral slope. Inserting into the expansion (12) thus yields the modal representation of the GM parameterized eddy-induced transport

$$\Upsilon^{\text{GM}} = -\frac{1}{\rho_o} \sum_{m=1}^{\infty} S_m(z) \left(\int_{-H}^0 dz' \kappa \nabla_z \rho S_m \right). \quad (14)$$

If the eddy fluxes are indeed dominated by low baroclinic modes, as argued in Section 2.2, we might attempt to approximate the expansion (11) by a low-order truncation, the severest of which is

$$\Upsilon^{\text{GM}} \approx S_1(z) \Upsilon_1(x, y, t). \quad (15)$$

In addition, in such a scheme the diffusivity κ must be depth independent, because it parameterizes eddy stirring by the dominant barotropic eddy velocity as discussed in Section 2.2. (Formally κ must be set equal to zero right at the boundaries, so that Υ^{GM} satisfies the boundary conditions and can be projected on the S_m modes. This introduces a very small correction in practice.) The truncation (15) satisfies the required boundary conditions and, by construction, has a low mode structure. We have explored this approach, as well as higher order truncations, in various simulations (not shown), but found that it leads to a non-robust parameterization. The main problem lies in columns that have extended regions of low stratification, for which the series (14) converges very slowly.

3.2. The proposed boundary value problem

We now consider an alternative to the truncated modal expansion discussed above. Here, we construct a boundary value problem to effectively low-pass the eddy transport to retain only the lowest vertical modes. A similar approach was suggested by Sasaki (1970) in the context of variational assimilation, and Jackson et al. (2008) noted the utility of this approach for computing a diffusivity

used to parameterize shear-driven turbulence. Most relevant to our application, Killworth and Nurser (2006) proposed such a method to vertically smooth the parameterized mesoscale eddy transport arising from Gent et al. (1995) and to provide for straightforward satisfaction of the surface and bottom boundary conditions.

Our proposed one-dimensional boundary-value problem takes the form

$$\left(c^2 \frac{d^2}{dz^2} - N^2 \right) \tilde{\Upsilon} = (g/\rho_o) \kappa \nabla_z \rho \quad (16a, b)$$

$$\tilde{\Upsilon}(\eta) = \tilde{\Upsilon}(-H) = 0,$$

where c is a depth independent speed to be specified. The diffusivity κ is associated with the barotropic eddy stirring discussed by Smith and Vallis (2001), and reviewed in Section 2.2. We therefore consider this diffusivity to be depth independent from now on. (The absolute value and horizontal variation of κ may be chosen in a similar fashion to that used in traditional GM implementations.) Correspondingly, vertical structure to the parameterized transport $\tilde{\Upsilon}$ arises from the squared buoyancy frequency N^2 , and horizontal gradient of the density $\nabla_z \rho$. Homogeneous solutions (arising from setting the right hand side of Eq. (16) to zero) are exponential functions with a length scale set by c/N . Yet to satisfy the boundary conditions these functions must be set to zero. Thus, it is only the solution associated with the right hand side forcing that contributes to $\tilde{\Upsilon}$.

The term on the right hand side of Eq. (16a) is related to the GM transport by noting that $N^2 \Upsilon^{\text{GM}} = -(g/\rho_o) \kappa \nabla_z \rho$. Thus, when $c \rightarrow 0$, the parameterized transport $\tilde{\Upsilon}$ reduces to Υ^{GM} , except in thin boundary layers where $\tilde{\Upsilon}$ goes to zero while Υ^{GM} does not. More generally however, $\tilde{\Upsilon}$ has the desirable property of preferentially weighting the low vertical modes (Section 4.1).

One might consider dropping the N^2 term from Eq. (16a), in which case the formulation would reduce to one proposed by Aiki et al. (2004). Such a formulation would also enable boundary conditions to be satisfied and would smooth the GM transport. However, information about the background stratification, and hence about the mixed layer, would be lost. We thus do not consider this formulation further in this paper.

As we will expand upon in the subsequent discussion, formulation of the parameterization problem in terms of a boundary-value problem has a number of desirable properties, as follows.

- The new parameterized eddy-induced transport $\tilde{\Upsilon}$ reduces to the GM transport Υ^{GM} in the singular limit $c^2 \rightarrow 0$. For the general case of $c^2 > 0$, the second order differential operator in Eq. (16a) provides a means to satisfy the boundary conditions at the ocean top and bottom, without tapering or matching schemes required for Υ^{GM} .
- The boundary-value problem provides a filter to high vertical wave number structures (e.g., noise), as solutions preferentially weight the low modes, consistent with the physical picture of a transport with a grave vertical scale.
- The formulation interpolates through regions of vanishing stratification. No artificial floor on the value of N^2 , nor ceiling on the value of the neutral direction slope S , are required to regularize the transport. However, one related condition must be applied to the speed c , as discussed in Section 4.5.
- As for the Gent et al. (1995) scheme, as well as the class of schemes introduced by Aiki et al. (2004), the new parameterization provides a sign-definite sink for potential energy.
- Numerical implementation of the boundary-value problem (16) requires the solution of a tridiagonal problem for each vertical water column. Such problems are routinely handled by ocean models, and introduce trivial computational expense.

4. Properties and implementation

We now discuss properties of the parameterized eddy transport that arise from the boundary-value problem (16), and discuss numerical implementation choices.

4.1. Low pass modal filtering

Considering the special case of a rigid lid, we can express the solution to the boundary-value problem (16) as an expansion in terms of baroclinic modes

$$\tilde{\Upsilon} = \sum_{m=1}^{\infty} S_m(z) \tilde{\Upsilon}_m(x, y, t), \quad (17)$$

with the expansion coefficients determined by

$$\tilde{\Upsilon}_m = \frac{\Upsilon_m}{1 + (c/c_m)^2}, \quad (18)$$

where Υ_m are the expansion coefficients of the unfiltered eddy transport as given in Eq. (14). The denominator $1 + (c/c_m)^2$ acts as a quadratic low-pass filter, since the baroclinic gravity wave speeds c_m decrease as the mode number m increases ($c_{m+1} < c_m$). Hence, as desired, low baroclinic mode structures are preferentially weighted. We do note that our parameterization is not designed to capture submesoscale or surface trapped phenomena that may not be well represented by such baroclinic modes (Lapeyre, 2009).

4.2. Behaviour in weakly stratified regimes

So long as $c^2 > 0$, $\tilde{\Upsilon}$ will quadratically interpolate from a region where $N^2 > 0$ (e.g., ocean interior), through the region of $N^2 = 0$ (e.g., boundary layer). In particular, if $N^2 = 0$ in the surface mixed layer, $\tilde{\Upsilon}$ interpolates from its interior value to zero at the upper ocean boundary. That is to say, the second-order differential operator allows for $\tilde{\Upsilon}$ to smoothly transition between regions of varying buoyancy frequency. Note that if $c^2 = 0$ the parameterized transport $\tilde{\Upsilon}$ reduces to Υ^{GM} , which has problems with satisfying the boundary conditions, as discussed in Section 2.3.

The ability of $\tilde{\Upsilon}$ to interpolate through various regimes of stratification may be compared with the prescription of Ferrari et al. (2008), whose key ingredients are the following.

- (i) The eddy transport is linear in z within the surface mixed layer where $N^2 \approx 0$ and vanishes at the air-sea interface.
- (ii) The eddy transport transitions from its linear z -profile in the mixed layer to the interior GM profile (see Eq. (1)) through a transition layer. The transition layer is required, because eddy statistics transition smoothly from the mixed layer to the interior. The same applies to the bottom mixed layer.

The parameterized transport $\tilde{\Upsilon}$ arising from the boundary-value problem satisfies these properties, since the transport $\tilde{\Upsilon}$ vanishes at the ocean boundaries by construction, and it interpolates smoothly through weakly stratified mixed layers where N^2 is small and ρ is vertically homogeneous. Indeed, the scheme readily handles multiple regimes of weak stratification and determines the interpolation as a result of solving a one dimensional boundary-value problem, rather than by evaluating matching conditions based on an assumed vertical profile.

The interpolation through layers of weak stratification is formally quadratic in z (as follows from the solution of an equation of the form $c^2 d^2 \tilde{\Upsilon} / dz^2 = \text{constant}$), but if the layer is thinner than the vertical scale of the first baroclinic mode (or the mode at which the low-pass mode filter is active), then the solution of the boundary-value problem is essentially linear in z within the layer. If the

layer is very deep, the problem reduces to the spindown of a weakly stratified water column and the boundary-value problem is shown to perform very well in this case as well (see Section 5.1). Note that there is no need to deal explicitly with any transition layer that may exist beneath the mixed layer, because our low mode projection naturally avoids any sharp discontinuity in $\tilde{\Upsilon}$ at the mixed layer base.

In addition to proposing the use of boundary layer matching conditions at the ocean surface, Ferrari et al. (2008) propose boundary matching also at the ocean bottom. Conventional approaches can lead to excessive noise in the parameterized transport, arising from difficulties computing neutral slopes next to boundaries (i.e., truncated grid stencils) and from the often weak vertical stratification appearing in the deep ocean that leads to steep neutral directions. As the boundary-value problem method generally provides a smooth transition from the interior through the weak stratification in the abyss, it resolves these problems with the transport at the ocean bottom. We illustrate many of these effects in Section 5.4.

In boundary layers, especially the upper ocean mixed layer, the squared buoyancy frequency can be negative, since vertical mixing may incompletely stabilize gravitationally unstable parcels. Because we are interested in parameterizing mesoscale eddy transport arising from stably stratified ocean regions, we solve the boundary-value problem (16) with N^2 bounded from below, and specifically with $N^2 > N_0^2 > 0$. Doing so ensures that potential energy is always dissipated by the scheme (Section 4.3). We choose $N_0^2 = 10^{-24} \text{ sec}^{-2}$, which is close to numerical truncation levels.

4.3. Effects on potential energy

The GM parameterization provides a local sink of potential energy. We can verify this property by considering an adiabatic Bousinesq system with a linear equation of state, in which the domain integrated potential energy, $P = g \int \rho z dV$, evolves according to

$$\frac{\partial P}{\partial t} = g \int dV \frac{\partial \rho}{\partial t} z = g \int dV \Upsilon^{\text{GM}} \cdot \nabla_z \rho, \quad (19)$$

where we retain only the contribution to potential energy evolution from GM, with other contributions including the vertical advection of density by the mean circulation. The projection of the eddy-induced transport onto the horizontal density gradient is given by

$$g \Upsilon^{\text{GM}} \cdot \nabla_z \rho = -(\rho_0/\kappa) |N \Upsilon^{\text{GM}}|^2 \leq 0. \quad (20)$$

Hence, the GM scheme dissipates potential energy at each point in a stratified fluid; that is, it is a local sink.

The new scheme affects potential energy evolution according to

$$\frac{\partial P}{\partial t} = g \int dV \tilde{\Upsilon} \cdot \nabla_z \rho. \quad (21)$$

Use of the differential Eq. (16) renders

$$(g\kappa/\rho_0) \tilde{\Upsilon} \cdot \nabla_z \rho = -\left(N^2 |\tilde{\Upsilon}|^2 + c^2 |\tilde{\Upsilon}'|^2\right) + c^2 \frac{d}{dz} (\tilde{\Upsilon} \cdot \tilde{\Upsilon}'), \quad (22)$$

where primes are shorthand for a vertical derivative. Thus,

$$(g/\rho_0) \int dV \kappa \tilde{\Upsilon} \cdot \nabla_z \rho = - \int dV \left(N^2 |\tilde{\Upsilon}|^2 + c^2 |\tilde{\Upsilon}'|^2\right), \quad (23)$$

where the boundary conditions in Eq. (16b) allowed us to drop the total derivative upon vertically integrating over a column, and we recall that c^2 is assumed to be depth independent. The right hand side of Eq. (23) is negative semi-definite for all choices of the diffusivity $\kappa \geq 0$, which then proves

$$\frac{\partial P}{\partial t} = g \int dV \tilde{\Upsilon} \cdot \nabla_z \rho \leq 0. \quad (24)$$

Hence, the parameterized transport $\tilde{\Upsilon}$ arising from the boundary-value problem (16) also dissipates potential energy for each column. However, contrary to the GM scheme, the new scheme might not provide a potential energy sink at each grid point, since the total derivative in Eq. (22) is not sign-definite. It is only by integrating over a column that potential energy dissipation is ensured. This is perfectly acceptable behaviour from a physical standpoint because mesoscale eddies are not necessarily local sinks of potential energy, as found by Wolfe et al. (2008) in eddy resolving simulations. Furthermore, there are no numerical reasons to insist on local potential energy dissipation.

4.4. Effects on potential vorticity

Eddies are often assumed to transport potential vorticity down-gradient (e.g., Green, 1970; Rhines and Young, 1982), and we wish to see if our parameterization respects this property. Plumb and Ferrari (2005) show that the component of the potential vorticity flux directed against the mean potential vorticity gradient is well approximated by the horizontal quasi-geostrophic potential vorticity flux. From this perspective, an eddy parameterization should generate a quasi-geostrophic potential vorticity flux directed on average against the mean horizontal potential vorticity gradient. We now consider how the parameterized transport $\tilde{\Upsilon}$ affects the mean potential vorticity, and show under what assumptions it achieves the above mixing of potential vorticity.

In the ocean, the large-scale potential vorticity gradient in the horizontal is dominated by the stretching term (Smith, 2007) so that

$$\nabla_z q \approx -\frac{fg}{\rho_0} \frac{\partial}{\partial z} \left(\frac{\nabla_z \rho}{N^2}\right). \quad (25)$$

Now from (7) we have

$$\langle \mathbf{u}'q' \rangle \approx -f \partial_z \tilde{\Upsilon}, \quad (26)$$

and therefore

$$\nabla_z q \cdot \langle \mathbf{u}'q' \rangle = \frac{f^2 g}{\rho_0} \frac{\partial}{\partial z} \left(\frac{\nabla_z \rho}{N^2}\right) \cdot \partial_z \tilde{\Upsilon}. \quad (27)$$

Use of the boundary-value problem (16) to replace the horizontal density gradient yields

$$f^{-2} \nabla_z q \cdot \langle \mathbf{u}'q' \rangle \approx c^2 \frac{\partial}{\partial z} \left(\frac{\tilde{\Upsilon}' \cdot \tilde{\Upsilon}''}{\kappa N^2}\right) - \frac{c^2 |\tilde{\Upsilon}''|^2}{\kappa N^2} - \tilde{\Upsilon}' \cdot \frac{\partial}{\partial z} (\kappa^{-1} \tilde{\Upsilon}). \quad (28)$$

Consider first the special case with $c = 0$; this is the GM case in which $\tilde{\Upsilon} = \Upsilon^{\text{GM}} = -\kappa \mathbf{S}$ for which (28) becomes

$$f^{-2} \nabla_z q \cdot \langle \mathbf{u}'q' \rangle \approx -\partial_z (\kappa \tilde{\Upsilon}) \cdot \partial_z \tilde{\Upsilon}. \quad (29)$$

The parameterized potential vorticity flux is then guaranteed to be locally oriented down the mean potential vorticity gradient if the diffusivity κ is depth independent. This result is expected, for it is known that the GM parameterization is equivalent to a thickness transport if κ is vertically uniform (Treguier et al., 1997; Vallis, 2006), and a thickness transport is like a potential vorticity transport if the planetary and relative vorticities are small, as we have assumed. However, a problem arises in the implementation of the GM parameterization, because κ must be set equal to zero at the boundaries to guarantee that $\Upsilon^{\text{GM}} = 0$ there. This constraint then introduces depth dependence to κ , which means that the

parameterized thickness flux is not down to the mean potential vorticity gradient at the boundaries.

With $c > 0$, the first term on the right-hand side of Eq. (28) is not sign definite. Hence, the parameterized potential vorticity flux is not necessarily locally down-gradient. Vertical integration renders

$$\int_{-H}^0 \nabla_z q \cdot \langle \mathbf{u}'q' \rangle dz = \left[\frac{c^2 f^2}{\kappa N^2} \tilde{\Upsilon}' \cdot \tilde{\Upsilon}'' \right]_{-H}^0 + \mathcal{N}, \quad (30)$$

where \mathcal{N} is the vertical integral of the last two terms on right-hand side of Eq. (28). With κ depth-independent, \mathcal{N} is negative-definite. In the absence of horizontal density gradients at the boundaries, $\tilde{\Upsilon}''$ vanishes at the boundaries, as can be seen by inspection of the boundary-value problem (16) at $z = \eta, -H$. In this case, the potential vorticity flux is downgradient in a vertically integrated sense. However, in the presence of horizontal density gradients at the boundaries, which is common at the ocean surface, the boundary term on the right hand side of Eq. (30) is not sign definite and the sign of the potential vorticity flux is indefinite. In the linear Eady problem, discussed in Section 5.1, characterized by non-zero density gradients at the boundaries, the boundary terms on the right hand side of Eq. (30) exactly cancel \mathcal{N} . This cancellation arises since the potential vorticity flux is zero for the linear Eady problem. Much like in the GM formulation, our proposed boundary-value problem does not guarantee that the potential vorticity flux is downgradient in the more general case, neither locally nor in an integrated sense.

The presence of boundary terms on the right hand side of Eq. (30) may be related to the surface solutions described, e.g., by Lapeyre et al. (2006). Horizontal density gradients at the ocean surface support solutions other than the baroclinic eigenmodes $S_m(z)$ employed in this paper (see Appendix B). The eigenmodes $S_m(z)$ are a complete basis for square-integrable functions over an ocean column. Yet surface density gradients, which may be regarded as a delta-function contributions to potential vorticity in the quasi-geostrophic approximation, cannot be well represented by a finite number of $S_m(z)$ modes: the second derivative $\tilde{\Upsilon}''$ must be non-zero for buoyancy or potential vorticity fluxes to exist at the ocean boundaries, but $S_m'' = 0$ there. Thus, in the presence of surface density gradients, additional surface solutions should be considered to properly represent the surface fluxes. We do not explore this possibility further in this paper, noting that the observational evidence that the ocean kinetic energy is indeed trapped in low baroclinic modes Wunsch (1997) suggests that surface solutions do not in practice fundamentally alter our overall picture. Nevertheless, the role of surface solutions in mixing of potential vorticity and its implications for eddy parameterizations are certainly worthy of future study.

4.5. Specifying the squared speed c^2

Fully specifying the boundary-value problem (16) requires a prescription for the squared speed c^2 weighting the second order differential operator. Given the dominance of low baroclinic mode features in mesoscale eddies, a natural approach is to set $c = c_M$ for a low baroclinic mode M , such as $c = c_1$ the first baroclinic gravity wave speed. This setting is further motivated by the example of the Eady problem considered in Section 5.1. The boundary-value problem with $c = c_1$ low-passes the baroclinic coefficients in the expansion of $\tilde{\Upsilon}$ in Eq. (18) as

$$\tilde{\Upsilon}_m = \frac{\Upsilon_m}{1 + m^2}, \quad (31)$$

where we used the WKB expression for the baroclinic gravity wave speeds given in Appendix B (see Eq. (60)). The filter thus acts on all

modes $m > 1$ and has a rolloff of m^{-2} . We now consider some practical issues with regards to this recommendation.

4.5.1. Amplitude of the parameterized transport

The first consideration concerns the amplitude of the transport $\tilde{\Upsilon}$ with $c = c_1$. From the expansion coefficients (31), ignoring all higher order terms (which vanish if the vertical structure is first baroclinic mode), the boundary-value problem transport is one-half the size of the truncated transport $\Upsilon_{\text{truncate}}^{\text{GM}}$ given by (15). This reduced amplitude accounts for the reduced scale in the eddy-induced overturning streamfunctions from the realistic numerical simulations shown in Section 5.4 with $c = c_1$. This magnitude difference affects our ability to perform a direct comparison to experiments run with Υ^{GM} . One means to reduce the amplitude difference is to set $c = c_M$, with $M > 1$. This choice still leads to a dominance of the first baroclinic mode for determining the structure of the transport. Setting $M = 2$, for example, leads to

$$\tilde{\Upsilon} = \sum_{m=1}^{\infty} S_m(z) \tilde{\Upsilon}_m(x, y, t) = \frac{S_1(z) \Upsilon_1}{1 + 1/4} + \sum_{m=2}^{\infty} \frac{S_m(z) \Upsilon_m(x, y, t)}{1 + (m/2)^2}. \quad (32)$$

Furthermore, setting $c = c_M$ with $M > 1$ does not necessarily admit higher modes to $\tilde{\Upsilon}$, since the expansion functions Υ_m will be non-trivial only when $\kappa \nabla_z \rho$ has a nontrivial projection onto higher modes. Hence, $M > 1$ is still consistent with low modes dominating the transport, as suggested by Smith and Vallis (2002).

4.5.2. Setting a minimum for the speed

A second practical issue arises in the implementation of the boundary-value problem with c set by a baroclinic gravity wave speed $c = c_M$. In regions where the whole water column is weakly stratified, the magnitude of the eddy transport $\tilde{\Upsilon}$ can become very large. Consider the limiting case with constant vertical stratification so that $N = \text{constant}$. The constant stratification case is considered by Eady (1949) and discussed in more detail in Section 5.1. In this case with $c = c_M$, the boundary-value problem reduces to

$$N^2 \left(\frac{H^2}{M^2 \pi^2} \frac{d^2}{dz^2} - 1 \right) \tilde{\Upsilon} = (g/\rho_o) \kappa \nabla_z \rho, \quad (33)$$

where $c_M = NH/(M\pi)$ with a constant stratification (see Eq. (62d) in Appendix B). If the right-hand side of Eq. (16) remains finite, then the magnitude of $\tilde{\Upsilon}$ grows without bound as $N \rightarrow 0$. Although it may be possible to obviate this problem with a judicious choice of the diffusivity κ , a simpler recipe to keep the magnitude of $\tilde{\Upsilon}$ bounded in such regions is to set a minimum value for c

$$c = \max[c_{\text{min}}, c_M], \quad (34)$$

where c_M is the chosen baroclinic gravity wave speed determined for each water column, and c_{min} is a constant. A similar problem arises in the implementation of the GM parameterization where an upper bound of the isopycnal slope is often imposed to keep the streamfunction bounded.

A related difficulty may also arise in the numerical solution of (16). The differential equation gives rise to the length scale c/N , and this length should be resolved by the model grid; that is, we require $\Delta z < c/N$. Now, c_m scales with the average value of N so that if there are regions of high stratification overlying a deep unstratified abyss then c_M may be small in regions where N is large, so that satisfaction of the above inequality may require a finer grid than might otherwise be chosen. A solution again is to set a minimum value of c , as in Eq. (34).

5. Examples of parameterized transport

We consider various examples that compare the streamfunction computed using our proposed boundary-value problem (16) and more conventional approaches using the GM scheme.

5.1. A nonlinear Eady problem

The linear Eady problem is a classic example of the release of potential energy through baroclinic instability and associated eddy transport (Eady, 1949). Eady considered an adiabatic Boussinesq fluid on an f -plane with constant depth H confined between two rigid plates at $z = 0$ and $z = -H$. The prescribed basic state has a uniform vertical stratification ($N^2 = \text{constant}$) along with a constant horizontal density gradient in thermal wind balance with a jet so that

$$\rho_0 f \partial_z \mathbf{u} = -g \hat{\mathbf{z}} \wedge \nabla \rho = \text{constant}. \quad (35)$$

This configuration is baroclinically unstable and leads to the spontaneous development of exponentially growing baroclinic eddies that act to tilt the density surfaces towards the horizontal, releasing available potential energy and resulting in an increase of vertical stratification.

Fox-Kemper et al. (2008) studied the nonlinear spindown of the basic state considered by Eady, but used a primitive equation model rather than the quasi-geostrophic system considered by Eady. As soon as baroclinic instability develops, baroclinic fronts slump from the vertical to the horizontal. The spindown is well described by a constant transport of the form (see equation (20) in Fox-Kemper et al., 2008),

$$\mathbf{Y}^{\text{Eady}} = -C_e \left(\frac{(HN)^2}{|f|} \right) \mathbf{S} \mu(z), \quad (36)$$

with $C_e = 0.06$ and where

$$\mu(z) = \left[1 - \left(\frac{2z}{H} + 1 \right)^2 \right] \left[1 + \frac{5}{21} \left(\frac{2z}{H} + 1 \right)^2 \right] \quad (37)$$

is a dimensionless function of first baroclinic mode structure that vanishes at the top $z = 0$ and bottom $z = -H$ boundaries. Fox-Kemper et al. (2008) tested this scaling with a large suite of numerical simulations to explore the full parameter space. We now investigate how the eddy-induced transports from Gent et al. (1995) and the new boundary value method compare to the scaling law (37).

When applied to the stratification for the nonlinear Eady problem, the GM parameterization gives a constant eddy transport since the density slope is constant, $\mathbf{Y}^{\text{GM}} = -\kappa \mathbf{S}$. This transport results in zero horizontal eddy advection in the water column: $\mathbf{u}^{\text{GM}} = -\partial_z \mathbf{Y}^{\text{GM}} = 0$. To satisfy the surface and bottom boundary conditions, the transport must jump to zero at $z = 0$ and $z = -H$, thus taking the form of a step function whose vertical derivative yields delta-function jets at the boundaries. These spurious boundary jets are absent in the analytic-numeric result (36), and methods to smoothly transition towards the boundary, such as Ferrari et al. (2008), are only partially able to ameliorate this fundamentally incorrect behaviour of the GM parameterization for the nonlinear Eady problem. A reviewer pointed out that our characterization of the GM streamfunction is not unique. Streamfunctions are defined up to an arbitrary constant. For the Eady problem the GM streamfunction is a constant and could be set to zero to satisfy the top and bottom boundary conditions. With this choice $\mathbf{u}^{\text{GM}} = 0$ everywhere with no need of delta-function jets at the boundaries. This solution, however, is physically unsatisfactory in the following sense: the Eady front does slump from the vertical to the horizontal during the nonlinear spindown, and this can only be achieved with a non-zero eddy advection.

We may analytically solve the boundary-value problem in Eq. (16) for constant density gradients in the vertical and horizontal, and depth independent diffusivity κ . In this case, the parameterized transport takes the form

$$\tilde{\mathbf{Y}}^{\text{Eady}} = -\kappa \mathbf{S} \tilde{\mu}, \quad (38)$$

where $\tilde{\mu}$ is a dimensionless structure function defined by Eq. (68) in Appendix B.2. When the speed c for the boundary-value problem is taken as the first baroclinic phase $c = NH/\pi$ for the Eady problem, then the structure function takes the form

$$\tilde{\mu}_{c_1} = 1 - \frac{\cosh[(\pi/2)(2z/H + 1)]}{\cosh(\pi/2)}. \quad (39)$$

In this case, Fig. 1 shows there is a near exact agreement between the boundary-value problem structure function (39) and the structure function (37) from Fox-Kemper et al. (2008). In contrast, the step-like structure function from GM is qualitatively distinct. We also show the structure function (68) for $c = c_2 = NH/2\pi$ and $c = c_4 = NH/4\pi$, each of which deviate from the Fox-Kemper et al. (2008) structure function (37), further supporting the use of $c = c_1$ for the boundary-value problem.

The agreement with the structure function from the numerical solutions from Fox-Kemper et al. (2008) suggests that the boundary-value problem approach is capturing the non-local behavior of eddy fluxes in the vertical, and generates a sheared eddy transport that restratifies the whole water column. Traditional GM approaches fail to produce restratification in the nonlinear Eady problem. Whether similar differences carry over to more complex flows remains to be explored.

Fox-Kemper et al. (2008) point out that the eddy fluxes of density can be split into two components with different effects on the evolution of the Eady front. There is an advective component dominated by low modes which drives the frontal slumping and restratification. This is the component captured by the boundary-value problem. In addition, there is a diffusive component that acts to slightly spread the front laterally by mixing density in the horizontal. This second component has little overall effect on the evolution of the front, but it is associated with non-zero surface density fluctuations. A careful exploration of these effects might shed light in how to incorporate in the parameterization the effect of the surface solutions alluded to in Section 4.4.

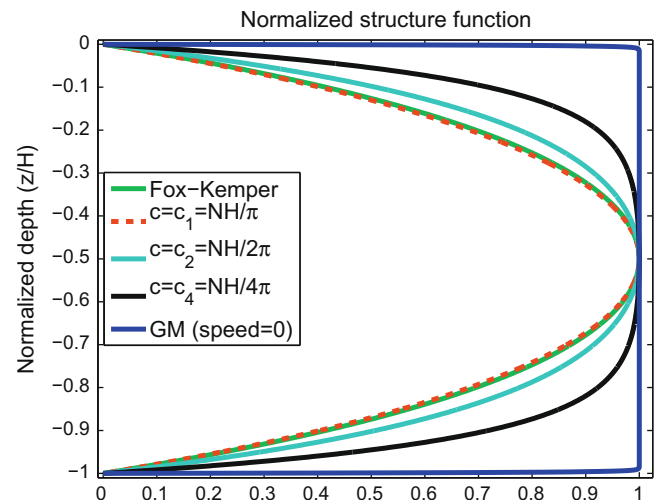


Fig. 1. Eddy transport structure functions for the Eady problem, normalized by their respective maximum values and shown over a normalized depth range. The step-like function corresponds to the structure function for the GM scheme (with speed $c = 0$). The left-most dashed curve is actually two curves, with the structure function (37) from Fox-Kemper et al. (2008) overlying the structure function (39) from the boundary-value problem, where the boundary-value problem used a speed $c = c_1 = NH/\pi$ corresponding to the first baroclinic phase speed for the Eady problem. Two more curves are shown to the right of $c = c_1 = NH/\pi$, corresponding to the boundary-value problem structure function (68) (Appendix B.2) with lower mode phase speeds $c = c_2 = NH/2\pi$ and $c = c_4 = NH/4\pi$, thus illustrating that the fit to the Fox-Kemper et al. (2008) structure function is best for $c = c_1$.

5.2. Comments on the numerical simulations

For the two numerical examples presented in the remainder of this section, we use the MOM4 code of Griffies (2009), where the boundary-value problem method is compared to an implementation of the GM scheme in MOM4 of Gent and McWilliams (1990) according to the skew flux formulation of Griffies (1998), denoted GFDL-GM. For the GM approach, boundary layers are treated according to Ferrari et al. (2008), with details given in Appendix A.4. Alternative implementations, whose details may differ particularly in the boundary layers, will produce results that differ from the GM MOM4 simulations presented here. Nonetheless, since MOM4 has been used by numerous modellers, and its methods the subject of various published papers (e.g., Griffies et al., 1998; Griffies, 1998; Griffies et al., 2005; Gnanadesikan et al., 2007) and technical guides, it serves as a benchmark for us to compare the boundary-value problem approach proposed in this paper.

As a further caveat on the following results, we acknowledge that the numerical simulations are meant to provide a flavour for elements of the new boundary-value problem method. Extensive further study, both with realistic global climate simulations and idealized eddying models, is required to fully assess the merits of the new approach.

5.3. Idealized numerical model configuration

We consider an idealized model ocean consisting of a flat-bottom southern hemisphere sector-channel configuration, containing both a re-entrant channel and a subtropical gyre, forced by wind and surface density gradients. We choose the same geometry and forcing as Zhao and Vallis (2008), though modify particulars of the parameterizations as follows. As in Ferrari et al. (2008), we impose an upper ocean mixed layer by introducing large vertical tracer diffusivity and frictional viscosity with values $10^{-3} \text{ m}^2 \text{ s}^{-1}$ over the upper 180 m. Beneath this layer, the diffusivity is exponentially reduced to $2 \times 10^{-5} \text{ m}^2 \text{ s}^{-1}$ and viscosity is reduced to $2 \times 10^{-4} \text{ m}^2 \text{ s}^{-1}$.

Fig. 2 shows the eddy-induced meridional overturning streamfunction (see Eq. (51) in Appendix A.2) computed using three different approaches, each time averaged over simulation years 901–1000. The left panel results from the more conventional GFDL-GM MOM4 method. The middle panel shows the streamfunction resulting from solving the boundary-value problem (16) at each model time step, with the speed weighting the second order operator equal to the first baroclinic phase speed, $c = c_1$. We also choose the minimum speed as $c_{\min} = 0.1 \text{ m/s}$. The right panel chooses $c_{\min} = 1.0 \text{ m/s}$.

Of particular note in the two boundary-value problem simulations is the absence of the higher mode structure found in the GFDL-GM MOM4 method. The filtering of such higher mode structure was anticipated by the discussion in Section 4.5. There is, however, some sensitivity to the choice of speed to weight the second order operator. This sensitivity arises since a large fraction of the southern region in the model domain is dominated by unstratified water all the way to the ocean bottom, in which case the baroclinic phase speeds approach zero. Such sensitivity is greater than seen in the realistic case considered in Section 5.4. But as a test of the fundamental numerical stability of the scheme, and overall structure of the overturning circulation, we conclude that the new scheme is indeed numerically stable (the simulations were run for 1000 years with no sign of instability); and that it performs in a manner consistent with the theoretical arguments presented in Section 4.

5.4. Realistic global model configuration

Our second numerical example is from a global ocean–ice model using the Normal Year Forcing from Large and Yeager (2004), and the experimental design and MOM4 configuration detailed in Griffies et al. (2005, 2009). We integrate the model for one year, starting from the temperature and salinity climatology of Steele et al. (2001). The evolution from the initial state is small, so that the simulation effectively provides a diagnosis for the streamfunctions occurring when the density field closely corresponds to climatology.

Fig. 3 shows the eddy-induced meridional overturning streamfunction (see Eq. (51) in Appendix A.2) arising from the more conventional GFDL-GM MOM4 method, and various approaches to the boundary value method. We show the eddy-induced meridional overturning streamfunction only in the Southern Ocean, since values to the north are generally quite small.

Each method results in similar qualitative features, yet the magnitudes differ especially for the case with $c = c_1$, which results from the scaling discussed in Section 4.5. Use of the higher wave speeds allows for more structure in the vertical, especially seen in the northern region. As for the idealized test in Section 5.3, we see how the boundary-value problem method acts to filter higher mode structures. Additionally, sensitivity of the boundary-value problem method to the minimum phase speed c_{\min} is far less than for the idealized configuration. The reduced sensitivity arises since there are fewer regions in the realistic case that exhibit fully unstratified water columns.

As anticipated in Section 4.2, examination of the streamfunction reveals that the boundary-value method produces a smoother re-

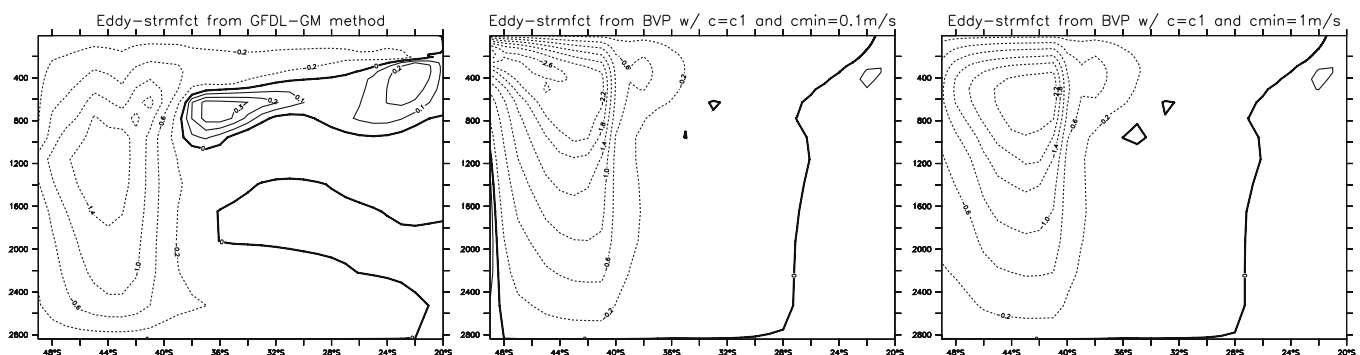


Fig. 2. Eddy-induced meridional overturning streamfunction (Eq. (51)) derived from three different approaches in the southern hemisphere sector-channel configuration, as time averaged over years 901–1000. Left panel: GFDL-GM MOM4 method (note that Zhao and Vallis (2008) integrate their simulations for 10,000 years, which explains the distinction with the solution shown here and their Figure 4). Middle panel: boundary-value problem method defined by Eq. (16) using the specification (34) with $c = c_1$ (first baroclinic phase speed) and $c_{\min} = 0.1 \text{ m/s}$. Right panel: boundary-value problem method defined by Eq. (16) using the specification (34) with $c = c_1$ and $c_{\min} = 1 \text{ m/s}$.

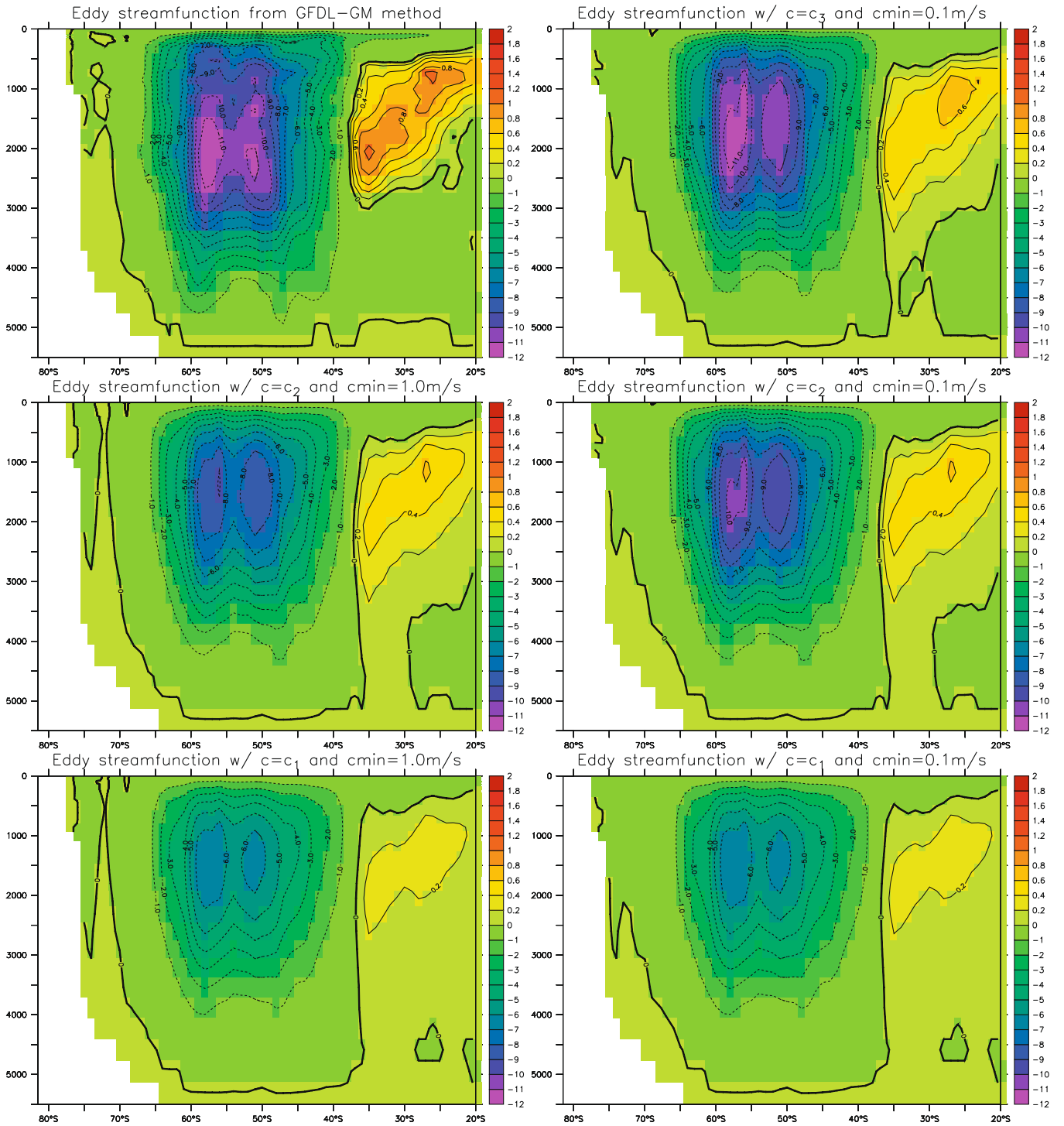


Fig. 3. Eddy-induced meridional overturning streamfunction (Eq. (51)) in the Southern Ocean for the global ocean–ice configuration. The results are time averaged over the first year of integration, starting from Steele et al. (2001). Note the different contour intervals for the negative versus positive streamfunction values. Top left panel: GFDL-GM method. Top right panel: boundary-value problem method with $c = c_3$ (third baroclinic gravity wave speed) and $c_{min} = 0.1$ m/s. Middle left panel: boundary-value problem method with $c = c_2$ and $c_{min} = 1.0$ m/s. Middle right panel: boundary-value problem method with $c = c_2$ and $c_{min} = 0.1$ m/s. Bottom left panel: boundary-value problem method with $c = c_1$ and $c_{min} = 1$ m/s. Bottom right panel: boundary-value problem method with $c = c_1$ and $c_{min} = 0.1$ m/s.

sult throughout the domain, especially in regions of steep neutral slopes and near the bottom. We illustrate this feature in Fig. 4, which shows the meridional eddy-induced transport at 60°E (Indian sector of Southern Ocean) for the case with $c = c_1$ and $c_{min} = 0.1$ m/s. The absence of a zonal integral (which can serve as a smoothing operation) reveals the added (arguably spurious) structure resulting from the GFDL-GM MOM4 method. The bound-

ary-value problem solution, in contrast, is significantly smoother, reflecting the large-scale effects arising from the stratification in the column, rather than exposing the streamfunction to the fine scale details of the local stratification. Similar results are found for the other streamfunctions (determined using different phase speeds) resulting from the boundary value problem method. Such a filtered parameterization of mesoscale eddy stirring near topog-

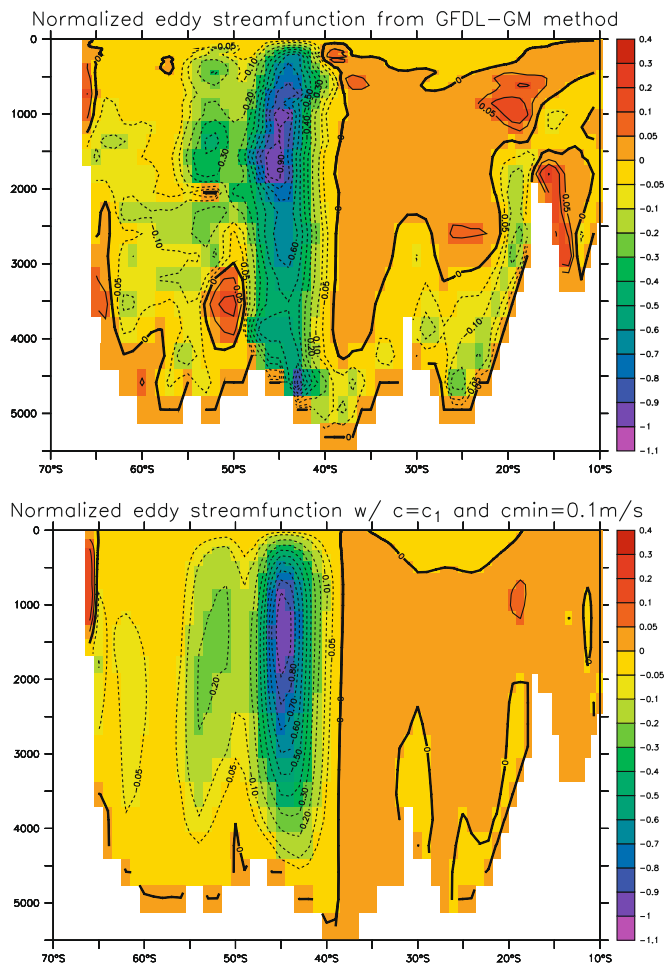


Fig. 4. Eddy-induced streamfunction at 60°E (Indian sector of Southern Ocean), derived from the GFDL-GM method (top) and boundary-value method (lower panel), with $c = c_1$ and $c_{\min} = 0.1$ m/s). The streamfunctions were normalized by their respective maximum absolute values along this section to facilitate plotting with a common colour bar. The results are time averaged over the first year of integration, starting from Steele et al. (2001). Note the smoother fields, especially near the ocean bottom.

raphy enhances our ability to cleanly examine other physical processes, such as breaking gravity waves, active in the abyss. However, in the absence of a clean comparison with eddy resolving simulations, no definitive statement can be made as to which eddy parameterization is objectively better.

6. Discussion and conclusions

Most current methods of computing the parameterized meso-scale eddy-induced streamfunction in numerical ocean climate models are based on the GM scheme (Gent and McWilliams, 1990; Gent et al., 1995). This scheme provides an eddy-induced stirring of tracers via a parameterized streamfunction, with the streamfunction parameterized with a local diffusive closure. Although this method has been successful in model applications, its implementation is not without difficulties. In particular, the parameterized eddy-induced transport $\Upsilon^{\text{GM}} = -\kappa \mathbf{S}$ must be interpolated through regions of weak vertical stratification, where the neutral slope \mathbf{S} can become infinite, and, relatedly, some form of tapering must be imposed to satisfy boundary conditions of zero transport at the top and bottom of the ocean. In addition, the scheme does not take advantage of the known phenomenology of mesoscale eddies in evolving toward larger vertical scales.

In order to overcome these difficulties we propose that the eddy-induced streamfunction may be computed as the solution to a one-dimensional boundary-value problem, (16), over each column of ocean fluid. The boundary-value problem provides a vertical filtering of the streamfunction that, in accord with earlier theoretical and numerical investigations by Smith and Vallis (2002), results in a transport streamfunction dominated by low vertical modes. The scheme satisfies appropriate boundary conditions at the top and bottom of the water column, and interpolates through multiple weakly stratified regions.

We summarize our investigation by listing what we see as the important attributes of the scheme.

- (i) For the Eady problem, the eddy-induced streamfunction arising from the boundary-value problem is nearly indistinguishable from the analytic-numeric results from Fox-Kemper et al. (2008), whereas the GM transport is qualitatively distinct.
- (ii) The boundary-value problem provides a low-pass filter with solutions preferentially weighting the low baroclinic modes, consistent with the phenomenology of geostrophic turbulence.
- (iii) As the boundary-value problem involves a second order differential operator (see Eq. (16)), homogeneous Dirichlet boundary conditions applied to the parameterized transport at the ocean top and bottom are implemented without tapering schemes.
- (iv) The parameterized eddy transport interpolates through regions of arbitrarily weak stratification, without a ceiling on the value of the neutral slope \mathbf{S} . However, in practice a minimum value for the speed, c , must be set, and the choice of c may be important in regions of uniformly weak stratification, though realistic tests performed thus far show only very weak sensitivity.
- (v) As for the Gent et al. (1995) scheme, as well as the generalized schemes introduced by Aiki et al. (2004), the new parameterization provides a sign-definite sink for potential energy. However, the new scheme provides a non-local sink in the vertical, which contrasts to the local sink of Gent et al. (1995).
- (vi) Numerical implementation of the boundary-value problem (16) requires the solution of a tridiagonal problem for each vertical column, with methods for such solutions straightforward and computationally inexpensive.

We have performed some preliminary numerical tests of this scheme, and compared it to an implementation of the GM scheme in MOM4 with boundary layer treatment according to Ferrari et al. (2008). We have not performed a detailed comparison, but our results suggest that the new scheme performs robustly, with no numerical instabilities, and that the eddy fluxes are largely consistent with the theoretical expectations listed above. Thus far, our scheme performs as well as our implementation of the more conventional GM scheme. Extensive further study is required to fully assess the merits and limitations of the new approach. In particular, the utility of a parameterization that emphasizes just the low modes need to be fully tested using both comprehensive global models and eddy primitive equation simulations.

Acknowledgements

We thank Alistair Adcroft, Gokhan Danabasoglu, Baylor Fox-Kemper, Peter Gent, Bob Hallberg, Isaac Held, Jim McWilliams, Maxim Nikurashin, Shafer Smith, Jan Zika, and an anonymous reviewer for discussions and comments that greatly improved the presentation. We dedicate this paper to the memory of Peter

Killworth. We would like to think that he would have found the approach to be of great interest, especially given the initial results from Killworth and Nurser (2006) indicating that he was thinking along similar lines, and we acknowledge his work in this area. RF acknowledges the support of NSF award OCE-0825376 and GKV acknowledges the support of NOAA.

Appendix A. Details of the fluxes and transport

The purpose of this appendix is to summarize salient points regarding the eddy-induced streamfunction and transport, formulation of the skew tracer fluxes, and implementation of the Ferrari et al. (2008) scheme.

A.1. The TRM streamfunction

The TRM method (see, e.g., McDougall and McIntosh, 2001; Nurser and Lee, 2004; Aiki et al., 2004; Eden et al., 2007; Aiki and Richards, 2008) is based on averaging the equations in density coordinates, i.e. using density as the vertical coordinate. The averaged equations are then converted back to (x, y, z) . To leading order in fluctuation amplitude, the TRM transport (referred to as the *quasi-Stokes* transport by McDougall and McIntosh (2001)) is given by the sum of two terms

$$\mathbf{\Upsilon}^{\text{TRM}} \approx \frac{\langle \mathbf{u}' \rho' \rangle}{|\partial_z \bar{\rho}|} + \frac{1}{2} \frac{\langle (\rho')^2 \rangle \partial_z \langle \mathbf{u} \rangle}{|\partial_z \bar{\rho}|^2}, \quad (40)$$

where $\bar{\rho}$ is the modified mean potential density (see for details, McDougall and McIntosh, 2001). The second term on the right hand side of Eq. (40) is dropped in the quasi-geostrophic limit (Plumb, 1990), in which case the TRM and TEM expressions are the same. By its definition, the unapproximated form of $\mathbf{\Upsilon}^{\text{TRM}}$ vanishes at the top and bottom boundaries (McDougall and McIntosh, 2001)

$$\mathbf{\Upsilon}^{\text{TRM}}(\eta) = \mathbf{\Upsilon}^{\text{TRM}}(-H) = 0, \quad (41)$$

where $z = \eta(x, y, t)$ is the ocean free surface, and $z = -H(x, y)$ is the solid-earth lower boundary. As discussed in Section 2.3, this Dirichlet boundary condition is employed by all parameterizations of the eddy-induced transport.

A.2. eddy-induced streamfunction and transport

There are two equivalent methods to incorporate the effects of SGS eddies parameterized by \mathbf{v}^* as given by Eq. (2). The first method stirs tracers via an additional advective transport, so that the material evolution of tracer concentration in a coarse resolution simulation is given by

$$\frac{dC}{dt} = -\nabla \cdot (\mathbf{v}^* C) - \nabla \cdot \mathbf{D}, \quad (42)$$

with \mathbf{D} parameterizing other SGS processes, such as diffusion. The second method represents the stirring through skewness using the vector streamfunction Ψ (Griffies, 1998; McDougall and McIntosh, 2001), so that

$$\frac{dC}{dt} = \nabla \cdot (\nabla C \wedge \Psi) - \nabla \cdot \mathbf{D}, \quad (43)$$

with

$$\mathbf{v}^* = \nabla \wedge \Psi. \quad (44)$$

The effects on the material evolution of tracer are the same whether stirring with advective fluxes or skew fluxes, and we see the equivalence by noting that the advective flux $\mathbf{v}^* C$ and skew flux $-\nabla C \wedge \Psi$ differ by a rotational flux that vanishes upon taking the divergence

$$\mathbf{v}^* C = -\nabla C \wedge \Psi + \nabla \wedge (C \Psi). \quad (45)$$

Whether one chooses to represent SGS stirring via advection or skewness is a matter of convenience. What is fundamental is that the parameterization of SGS tracer stirring reduces to a specification of the streamfunction Ψ . For convenience, we write

$$\Psi = \Upsilon \wedge \hat{z}, \quad (46)$$

where Υ is the parameterized eddy-induced transport.

The parameterized eddy-induced transport from Gent et al. (1995)

$$\Upsilon^{\text{GM}} = -\kappa \mathbf{S}, \quad (47)$$

requires computation of the neutral slope relative to the horizontal

$$\mathbf{S} = -\left(\frac{\nabla_z \rho}{\partial_z \rho} \right), \quad (48a)$$

$$= -\left(\frac{\rho_\theta \nabla_z \theta + \rho_S \nabla_z S}{\rho_\theta \partial_z \theta + \rho_S \partial_z S} \right), \quad (48b)$$

$$= -\left(\frac{\nabla_z B}{N^2} \right), \quad (48c)$$

where ∇_z is the horizontal gradient operator, ρ is the locally referenced potential density, θ is the potential temperature, S is the salinity,

$$B = -(g/\rho_0) \rho \quad (49)$$

is the buoyancy,

$$N^2 = \partial_z B \quad (50)$$

is the squared buoyancy frequency, and $\rho_\theta = \partial \rho / \partial \theta$ and $\rho_S = \partial \rho / \partial S$. The parameterized transport (47) reduces baroclinicity by flattening slopes, with the tendency for flattening strengthened in regions of steep neutral slopes.

The eddy-induced meridional volume transport (i.e., the eddy-induced meridional overturning streamfunction) passing beneath an arbitrary depth z , zonally integrated within a basin or over the globe, is computed by the integral

$$\mathcal{T}^{(y)}(y, z, t) = - \int dx \int_{-H}^z dz' v^* = - \int dx \Upsilon^{(y)}(x, y, z, t). \quad (51)$$

This transport is shown in Figs. 2 and 3 for the two numerical examples considered in the main text.

A.3. Skew tracer flux components

We follow the approach of Griffies (1998) by computing the effects on tracers from the parameterized eddy-induced transport via skew diffusion, as defined by an anti-symmetric stirring tensor

$$\mathbf{A} = \begin{pmatrix} 0 & 0 & \Upsilon^{(x)} \\ 0 & 0 & \Upsilon^{(y)} \\ -\Upsilon^{(x)} & -\Upsilon^{(y)} & 0 \end{pmatrix}, \quad (52)$$

acting on the gradient of the tracer concentration ∇C . The corresponding skew tracer flux is given by

$$\mathbf{F} = -\mathbf{A} \cdot \nabla C, \quad (53)$$

which has the following horizontal and vertical components

$$\mathbf{F}^{(h)} = -\Upsilon \partial_z C, \quad (54)$$

$$F^{(z)} = \Upsilon \cdot \nabla_z C. \quad (55)$$

We typically consider eddy-induced skew fluxes in concert with neutral diffusion, in which case the SGS transport tensor is the sum of the anti-symmetric tensor \mathbf{A} given by Eq. (52), and the symmetric small slope neutral diffusion tensor

$$\mathbf{K} = A_I \begin{pmatrix} 1 & 0 & S^{(x)} \\ 0 & 1 & S^{(y)} \\ S^{(x)} & S^{(y)} & S^2 \end{pmatrix}, \quad (56)$$

where A_I is the neutral diffusivity and $S^2 = \mathbf{S} \cdot \mathbf{S}$.

Some of the motivation for Griffies (1998) to use skew fluxes was to avoid problems associated with computing derivatives of the often numerically noisy transport $\Upsilon^{\text{GM}} = -\kappa \mathbf{S}$. The skew approach avoids such derivatives, and so provides a cleaner means for producing physically based results from the GM parameterization. However, given the more regular nature of $\tilde{\Upsilon}$, this motivation to implement the closure via skew fluxes is largely obsolete. One notable advantage of implementing the eddy closure as an advection operator is that one then may access from amongst the many monotonic advection schemes commonly used for tracer advection, with this approach originally proposed by Weaver and Eby (1997). In contrast, there is no analogous numerical scheme ensuring monotonic skew fluxes.

A.4. Implementation of Ferrari et al. (2008)

The purpose of this section is to summarize our implementation of the Ferrari et al. (2008) method used to transition the transport Υ^{GM} from the ocean interior through the surface boundary layer. Note that we do not implement a transition from the interior to the ocean bottom.

Our implementation simplifies the Ferrari et al. (2008) scheme by ignoring the postulated quadratic transition layer sitting between the surface mixed layer and the ocean interior. Instead, we transition directly from the base of the boundary layer to the ocean surface, with a linear depth dependence given to the streamfunction. As discussed by Danabasoglu et al. (2008), there is little sensitivity to the presence or absence of a transition region in realistic ocean configuration, so for purposes of this study, it is sufficient to use a simplified version of the algorithm. However, the transition layer stabilizes the algorithm and should be used in simulations where the surface mixed layer can become very shallow.

For determining the surface mixed layer depth for use in computing the transition of the streamfunction, we take the sum of the turbulent boundary layer determined by the upper ocean turbulence scheme, plus the thickness over which mesoscale eddies are thought to feel the base of the upper ocean turbulent mixed layer. The algorithm for computing the mesoscale eddy depth is taken from the appendix to Large et al. (1997), with further description given in Section 15.3.3 of Griffies (2004) and in Ferrari et al. (2008). For this calculation, we compute the product of the first baroclinic Rossby radius and the neutral slope, $\lambda_1 |\mathbf{S}|$. In the upper ocean turbulent boundary layer, where the neutral slopes are generally steep, $\lambda_1 |\mathbf{S}|$ is large. Starting from the surface, we search for the first depth D where $D > \lambda_1 |\mathbf{S}|$. This depth then determines the eddy depth.

Appendix B. Mathematical properties of baroclinic modes

This appendix summarizes some salient points regarding the baroclinic modes in linearized flat bottom primitive equations.

B.1. Baroclinic modes

As discussed in Section 6.11 of Gill (1982) and Section 4.2 of Philander (1990), the linearized, flat bottom, rigid lid, adiabatic, hydrostatic primitive equations admit an infinite number of mutually orthogonal eigenmodes that satisfy the following relations.

Pressure and horizontal velocity modes:

$$\frac{d}{dz} \left(\frac{1}{N^2} \frac{dR_m}{dz} \right) + \frac{1}{c_m^2} R_m = 0 \quad (57a)$$

$$\frac{d}{dz} R_m(0) = \frac{d}{dz} R_m(-H) = 0 \quad (57b)$$

$$\int_{-H}^0 dz R_m = 0 \quad (57c)$$

$$\left(\frac{g}{c_m^2} \right) \int_{-H}^0 dz R_m R_n = \delta_{mn} \quad (57d)$$

$$R_m = h_m \frac{dS_m}{dz} \quad (57e)$$

$$c_m^2 = gh_m \quad (57f)$$

$$R_m = \text{constant} \quad \text{if } N = 0 \quad (57g)$$

Vertical velocity modes:

$$\frac{d^2 S_m}{dz^2} + \left(\frac{N}{c_m} \right)^2 S_m = 0 \quad (58a)$$

$$S_m(0) = S_m(-H) = 0 \quad (58b)$$

$$g^{-1} \int_{-H}^0 dz N^2 S_m S_n = \delta_{mn} \quad (58c)$$

$$N^2 S_m = -g \frac{dR_m}{dz} \quad (58d)$$

$$S_m = 0 \quad \text{if } N = 0. \quad (58e)$$

As defined, both the horizontal velocity modes R_m and vertical velocity modes S_m are dimensionless. We make use of the vertical velocity modes S_m in Section 3, given the homogeneous Dirichlet boundary conditions; the vertical modes R_m would be appropriate for potential vorticity fluxes, and the two are related by $g dR_m/dz = -N^2 S_m$. Note that normalization results in an amplitude for S_m that is larger in regions of weak stratification where N is small. However, when $N = 0$ throughout the column, S_m vanishes.

A general buoyancy frequency requires a numerical solver to determine the eigenvalues and eigenmodes. However, as noted by Chelton et al. (1998), the WKB method can be used to approximate the baroclinic modes. They focus on the vertical velocity modes, in which case

$$S_m \approx S_m^0 \sin \left(\frac{1}{c_m} \int_{-H}^z N(z') dz' \right). \quad (59)$$

The vertical velocity baroclinic modes take the form of a stretched sine function, with stretching and zero crossings determined by the buoyancy frequency and wave speed c_m , where the baroclinic wave speeds are approximated by

$$c_m \approx (m\pi)^{-1} \int_{-H}^0 N dz. \quad (60)$$

In order to satisfy the normalization condition in Eq. (58e), the dimensionless normalization constant S_m^0 must have an inverse relation to the buoyancy frequency.

The WKB approximation for the horizontal velocity baroclinic mode R_m is determined by the relation $R_m = -h_m dS_m/dz$, so that

$$R_m \approx - \left(\frac{c_m N(z) S_m^0}{g} \right) \cos \left(\frac{1}{c_m} \int_{-H}^z N(z') dz' \right). \quad (61)$$

The case of uniform stratification with constant N corresponds to the Eady problem considered in Section 5.1. In this case, the normalized baroclinic modes take the form

$$N = \text{constant} \quad (62a)$$

$$S_m = \sqrt{\frac{2g}{HN^2}} \sin \left[(z+H) \frac{N}{c_m} \right] \quad (62b)$$

$$R_m = -\sqrt{\frac{2c_m^2}{gH}} \cos \left[(z+H) \frac{N}{c_m} \right] \quad (62c)$$

$$c_m = \frac{NH}{m\pi} \text{ for } m \geq 1. \quad (62d)$$

Notably, the buoyancy frequency appears in the denominator of the vertical velocity baroclinic modes, which allows these modes to satisfy the normalization condition in Eq. (58c).

B.2. Concerning completeness of the baroclinic modes

Within the quasi-geostrophic (QG) approximation, the dynamics are described by the distribution of the QG potential vorticity (PV)

$$q = f_0 + \beta y + \nabla^2 \phi + \frac{\partial}{\partial z} \left(\frac{f_0^2}{N^2} \frac{\partial \phi}{\partial z} \right) \quad -H < z < 0, \quad (63)$$

and the buoyancy at the top and bottom boundaries,

$$b = f_0 \frac{\partial \phi}{\partial z} \Big|_{z=0, -H}. \quad (64)$$

In these equations, $\nabla^2 = \partial^2/\partial x^2 + \partial^2/\partial y^2$ is the horizontal Laplacian operator; $-H \leq z \leq 0$ is a flat bottom ocean domain; $b = -g(\rho - \rho_0)/\rho_0$ is the buoyancy anomaly; ρ is the density; ρ_0 is a reference density; ϕ is the geostrophic streamfunction; f_0 is the Coriolis parameter at the latitude considered; and β is the planetary vorticity gradient. Bretherton (1966) shows that the elliptic problem for ϕ with non-homogeneous boundary conditions in Eqs. (63) and (64) is equivalent to the following elliptic problem with homogeneous boundary conditions,

$$q - (f_0/N)b_s \delta(z) = f_0 + \beta y + \nabla^2 \phi + \frac{\partial}{\partial z} \left(\frac{f_0^2}{N^2} \frac{\partial \phi}{\partial z} \right) \quad (65)$$

$$\partial_z \phi = 0, \quad z = 0, -H, \quad (66)$$

where the delta function represents the effect of surface buoyancy. The baroclinic modes R_m discussed in this appendix are a complete basis for this problem, because they satisfy the same boundary conditions over the ocean domain. Importantly, a basis is complete on the space of functions that may contain a finite number of discontinuities, but which are finite over the domain of interest. The functions ϕ, u, v, b satisfy such properties, and thus can be expressed as a linear combination of the baroclinic modes R_m and S_m . Hence, the buoyancy flux, and the associated eddy transport, can be expanded as a linear combination of S_m modes. However, PV is not such a function because of the delta function contribution at the boundary. The PV fluxes, thus, cannot generally be expanded in terms of the baroclinic modes. The eddy-induced velocity is another variable that cannot be expanded in baroclinic modes, because it depends on vertical derivatives of the streamfunction and can in theory have delta function contribution at the boundaries. High resolution numerical simulations, however, do not seem to produce eddy velocities with singular behavior at the boundaries.

Appendix C. Parameterized transport for the Eady problem

We present here the analytic solution to the boundary-value problem (16) for constant density gradients in the vertical and horizontal, and a depth independent diffusivity κ . This density field corresponds to the Eady problem discussed in Section 5.1. In this case, the boundary-value problem is a linear second order inhomogeneous differential equation. Standard analytical methods lead to the solution

geneous differential equation. Standard analytical methods lead to the solution

$$\tilde{\Upsilon} = -\kappa \mathbf{S} \tilde{\mu}, \quad (67)$$

where

$$\sinh(H/\lambda) \tilde{\mu}(z) = 2e^{-H/2\lambda} \sinh(z/\lambda) \sinh(H/2\lambda) - 2e^{z/2\lambda} \sinh(H/\lambda) \sinh(z/2\lambda) \quad (68)$$

defines a dimensionless structure function $\tilde{\mu}(z)$ over a vertical column, and

$$\lambda = c/N, \quad (69)$$

defines a length scale over which the structure function transitions from its maximum in the center of the column to its zero value at the boundaries. The $c \rightarrow 0$ limit corresponds to the Gent et al. (1995) scheme, in which case the structure function becomes a step function. Correspondingly, the parameterized eddy-induced velocity is a delta function at the top and bottom boundary when $c = 0$. In contrast, when $c = NH/\pi$, which is the first baroclinic phase speed when $N = \text{constant}$, the transition length scale is

$$\lambda_{c_1} = H/\pi, \quad (70)$$

which means the transition region extends well into the ocean interior.

References

- Aiki, H., Jacobson, T., Yamagata, T., 2004. Parameterizing ocean eddy transports from surface to bottom. *Journal of Geophysical Research* 31, L19 302. doi:10.1029/2004GL020703.
- Aiki, H., Richards, K., 2008. Energetics of the global ocean: the role of layer-thickness form drag. *Journal of Physical Oceanography* 38, 1845–1869.
- Andrews, D.G., McIntyre, M.E., 1978. Generalized Eliassen–Palm and Charney–Drazin theorems for waves on axisymmetric mean flows in compressible atmospheres. *Journal of Atmospheric Sciences* 35, 175–185.
- Bretherton, F.P., 1966. Critical layer instability in baroclinic flows. *Quarterly Journal of the Royal Meteorological Society* 92, 325–334.
- Charney, J.G., 1971. Geostrophic turbulence. *J. Atmos. Sci.* 28, 1087–1095.
- Chelton, D.B., DeSzoeke, R.A., Schlax, M.G., Naggar, K.E., Siwertz, N., 1998. Geographical variability of the first baroclinic Rossby radius of deformation. *Journal of Physical Oceanography* 28, 433–460.
- Danabasoglu, G., Ferrari, R., McWilliams, J., 2008. Sensitivity of an ocean general circulation model to a parameterization of near-surface eddy fluxes. *Journal of Climate* 21, 1192–1208.
- Eady, E., 1949. Long waves and cyclone waves. *Tellus* 1, 33–52.
- Eden, C., Greatbatch, R., 2008. Towards a mesoscale eddy closure. *Ocean Modelling* 20, 223–239.
- Eden, C., Greatbatch, R., Olbers, D., 2007. Interpreting eddy fluxes. *Journal of Physical Oceanography* 37, 1282–1296.
- Farneti, R., Delworth, T., Rosati, A., Griffies, S., Zeng, F., in press. The role of mesoscale eddies in the rectification of the Southern Ocean response to climate change. *Journal of Physical Oceanography*.
- Ferrari, R., McWilliams, J., Canuto, V., Dubovikov, M., 2008. Parameterization of eddy fluxes near oceanic boundaries. *Journal of Climate* 21, 2770–2789.
- Ferreira, D., Marshall, J., 2006. Formulation and implementation of a residual-mean ocean circulation model. *Ocean Modelling* 13, 86–107.
- Fox-Kemper, B., Ferrari, R., Hallberg, R., 2008. Parameterization of mixed layer eddies. I: theory and diagnosis. *Journal of Physical Oceanography* 38, 1145–1165.
- Gent, P.R., McWilliams, J.C., 1990. Isopycnal mixing in ocean circulation models. *Journal of Physical Oceanography* 20, 150–155.
- Gent, P.R., Willebrand, J., McDougall, T.J., McWilliams, J.C., 1995. Parameterizing eddy-induced tracer transports in ocean circulation models. *Journal of Physical Oceanography* 25, 463–474.
- Gill, A., 1982. *Atmosphere–ocean dynamics*. International Geophysics Series, vol. 30. Academic Press, London. pp. 662 + xv.
- Gnanadesikan, A., Griffies, S., Samuels, B., 2007. Effects in a climate model of slope tapering in neutral physics schemes. *Ocean Modelling* 17, 1–16.
- Green, J.S.A., 1970. Transfer properties of the large-scale eddies and the general circulation of the atmosphere. *Quart. J. Roy. Meteor. Soc.* 96, 157–185.
- Griffies, S.M., 1998. The Gent–McWilliams skew-flux. *Journal of Physical Oceanography* 28, 831–841.
- Griffies, S.M., 2004. *Fundamentals of Ocean Climate Models*. Princeton University Press, Princeton, USA. 518 + xxxiv.
- Griffies, S.M., 2009. Elements of MOM4p1. NOAA/Geophysical Fluid Dynamics Laboratory, Princeton, USA, p. 444.

- Griffies, S.M., Biastoch, A., Böning, C.W., Bryan, F., Chassignet, E., England, M., Gerdes, R., Haak, H., Hallberg, R.W., Hazeleger, W., Jungclaus, J., Large, W.G., Madec, G., Samuels, B.L., Scheinert, M., Gupta, A.S., Severijns, C.A., Simmons, H.L., Treguier, A.M., Winton, M., Yeager, S., Yin, J., 2009. Coordinated ocean–ice reference experiments (COREs). *Ocean Modelling* 26, 1–46.
- Griffies, S.M., Gnanadesikan, A., Dixon, K.W., Dunne, J.P., Gerdes, R., Harrison, M.J., Rosati, A., Russell, J., Samuels, B.L., Spelman, M.J., Winton, M., Zhang, R., 2005. Formulation of an ocean model for global climate simulations. *Ocean Science* 1, 45–79.
- Griffies, S.M., Gnanadesikan, A., Pacanowski, R.C., Larichev, V., Dukowicz, J.K., Smith, R.D., 1998. Isoneutral diffusion in a z-coordinate ocean model. *Journal of Physical Oceanography* 28, 805–830.
- Held, I.M., Larichev, V.D., 1996. A scaling theory for horizontally homogeneous baroclinically unstable flow on a beta plane. *Journal of Atmospheric Sciences* 53, 946–952.
- Jackson, L., Hallberg, R., Legg, S., 2008. A parameterization of shear-driven turbulence for ocean climate models. *Journal of Physical Oceanography* 38, 1033–1053.
- Killworth, P.D., Nurser, A., 2006. Implementing a nonlocal eddy parameterization into a global ocean model. *Geophysical Research Abstracts* 8, 10088.
- Klein, P., Hua, B.L., Lapeyre, G., Capet, X., Gentil, S.L., Sasaki, H., 2008. Upper ocean turbulence from high 3D resolution simulations. *Journal of Physical Oceanography* 38, 1748–1763.
- Lapeyre, G., 2009. What vertical mode does the altimeter reflect? on the decomposition in baroclinic modes and on a surface-trapped mode. *Journal of Physical Oceanography* 39, 2857–2874.
- Lapeyre, G., Klein, P., Hua, B.L., 2006. Oceanic restratification forced by surface frontogenesis. *Journal of Physical Oceanography* 36, 1577–1590.
- Large, W., Yeager, S., 2004. Diurnal to decadal global forcing for ocean and sea-ice models: the data sets and flux climatologies. NCAR Technical Note: NCAR/TN-460+STR. CGD Division of the National Center for Atmospheric Research.
- Large, W.G., Danabasoglu, G., Doney, S.C., McWilliams, J.C., 1997. Sensitivity to surface forcing and boundary layer mixing in a global ocean model: annual-mean climatology. *Journal of Physical Oceanography* 27, 2418–2447.
- McDougall, T.J., McIntosh, P.C., 2001. The temporal-residual-mean velocity. Part II: isopycnal interpretation and the tracer and momentum equations. *Journal of Physical Oceanography* 31, 1222–1246.
- Nurser, A.G., Lee, M.-M., 2004. Isopycnal averaging at constant height. Part II: relating to the residual streamfunction in Eulerian space. *Journal of Physical Oceanography* 34, 2740–2755.
- Philander, S.G., 1990. El Niño, La Niña, and the Southern Oscillation. Academic Press.
- Plumb, R., Ferrari, R., 2005. Transformed Eulerian mean theory. Part I: non-quasi-geostrophic theory for eddies on a zonal-mean flow. *Journal of Physical Oceanography* 35, 165–174.
- Plumb, R.A., 1990. A non-acceleration theorem for transient quasi-geostrophic disturbances on a three-dimensional time-mean flow. *Journal of Atmospheric Sciences* 47, 1825–1836.
- Rhines, P.B., Young, W.R., 1982. Homogenization of potential vorticity in planetary gyres. *Journal of Fluid Mechanics* 122, 347–367.
- Sasaki, Y., 1970. Some basic formalism in numerical variational analysis. *Monthly Weather Review* 98, 875–883.
- Smith, K.S., 2007. The geography of linear baroclinic instability in earth's oceans. *Journal of Marine Research* 65, 655–683.
- Smith, K.S., Vallis, G.K., 2001. The scales and equilibration of mid-ocean eddies: freely evolving flow. *Journal of Physical Oceanography* 31, 554–571.
- Smith, K.S., Vallis, G.K., 2002. The scales and equilibration of mid-ocean eddies: forced-dissipative flow. *Journal of Physical Oceanography* 32, 1669–1721.
- Steele, M., Morfey, R., Ermold, W., 2001. PHC: a global ocean hydrography with a high-quality Arctic Ocean. *Journal of Climate* 14, 2079–2087.
- Treguier, A.M., Held, I.M., Larichev, V.D., 1997. On the parameterization of quasi-geostrophic eddies in primitive equation ocean models. *Journal of Physical Oceanography* 27, 567–580.
- Vallis, G.K., 2006. *Atmospheric and Oceanic Fluid Dynamics: Fundamentals and Large-scale Circulation*. first ed.. Cambridge University Press, Cambridge. pp. 745 + xxv.
- Visbeck, M., Marshall, J.C., Jones, H., 1996. On the dynamics of convective “chimneys” in the ocean. *Journal of Physical Oceanography* 26, 1721–1734.
- Weaver, A.J., Eby, M., 1997. On the numerical implementation of advection schemes for use in conjunction with various mixing parameterizations in the GFDL ocean model. *Journal of Physical Oceanography* 27, 369–377.
- Wolfe, C.L., Cessi, P., McClean, J.L., Maltrud, M.E., 2008. Vertical heat transport in eddy ocean models. *Geophysics Research Letter* 35, L23605. doi:10.1029/2008GL036138.
- Wunsch, C., 1997. The vertical partition of oceanic horizontal kinetic energy and the spectrum of global variability. *Journal of Physical Oceanography* 27, 1770–1794.
- Zhao, R., Vallis, G.K., 2008. Parameterizing mesoscale eddies with residual and Eulerian schemes, and a comparison with eddy-permitting models. *Ocean Modelling* 23, 1–12.